Measurement of the forward-backward asymmetry in Λ_b^0 and $\overline{\Lambda}_b^0$ baryon production in $p\bar{p}$ collisions at $\sqrt{s} = 1.96$ TeV

V.M. Abazov,[31] B. Abbott,[67] B.S. Acharya,[25] M. Adams,[46] T. Adams,[44] J.P. Agnew,[41] G.D. Alexeev,[31]
G. Alkhazov,[35] A. Alton[a],[56] A. Askew,[44] S. Atkins,[54] K. Augsten,[7] C. Avila,[5] F. Badaud,[10] L. Bagby,[45]
B. Baldin,[45] D.V. Bandurin,[73] S. Banerjee,[25] E. Barberis,[55] P. Baringer,[53] J.F. Bartlett,[45] U. Bassler,[15]
V. Bazterra,[46] A. Bean,[53] M. Begalli,[2] L. Bellantoni,[45] S.B. Beri,[23] G. Bernardi,[14] R. Bernhard,[19] I. Bertram,[39]
M. Besançon,[15] R. Beuselinck,[40] P.C. Bhat,[45] S. Bhatia,[58] V. Bhatnagar,[23] G. Blazey,[47] S. Blessing,[44] K. Bloom,[59]
A. Boehnlein,[45] D. Boline,[64] E.E. Boos,[33] G. Borissov,[39] M. Borysova[l],[38] A. Brandt,[70] O. Brandt,[20] R. Brock,[57]
A. Bross,[45] D. Brown,[14] X.B. Bu,[45] M. Buehler,[45] V. Buescher,[21] V. Bunichev,[33] S. Burdin[b],[39] C.P. Buszello,[37]
E. Camacho-Pérez,[28] B.C.K. Casey,[45] H. Castilla-Valdez,[28] S. Caughron,[57] S. Chakrabarti,[64] K.M. Chan,[51]
A. Chandra,[72] E. Chapon,[15] G. Chen,[53] S.W. Cho,[27] S. Choi,[27] B. Choudhary,[24] S. Cihangir,[45] D. Claes,[59]
J. Clutter,[53] M. Cooke[k],[45] W.E. Cooper,[45] M. Corcoran,[72] F. Couderc,[15] M.-C. Cousinou,[12] D. Cutts,[69]
A. Das,[71] G. Davies,[40] S.J. de Jong,[29,30] E. De La Cruz-Burelo,[28] F. Déliot,[15] R. Demina,[63] D. Denisov,[45]
S.P. Denisov,[34] S. Desai,[45] C. Deterre[c],[41] K. DeVaughan,[59] H.T. Diehl,[45] M. Diesburg,[45] P.F. Ding,[41]
A. Dominguez,[59] A. Dubey,[24] L.V. Dudko,[33] A. Duperrin,[12] S. Dutt,[23] M. Eads,[47] D. Edmunds,[57] J. Ellison,[43]
V.D. Elvira,[45] Y. Enari,[14] H. Evans,[49] A. Evdokimov,[46] V.N. Evdokimov,[34] A. Fauré,[15] L. Feng,[47] T. Ferbel,[63]
F. Fiedler,[21] F. Filthaut,[29,30] W. Fisher,[57] H.E. Fisk,[45] M. Fortner,[47] H. Fox,[39] S. Fuess,[45] P.H. Garbincius,[45]
A. Garcia-Bellido,[63] J.A. García-González,[28] V. Gavrilov,[32] W. Geng,[12,57] C.E. Gerber,[46] Y. Gershtein,[60]
G. Ginther,[45,63] O. Gogota,[38] G. Golovanov,[31] P.D. Grannis,[64] S. Greder,[16] H. Greenlee,[45] G. Grenier,[17]
Ph. Gris,[10] J.-F. Grivaz,[13] A. Grohsjean[c],[15] S. Grünendahl,[45] M.W. Grünewald,[26] T. Guillemin,[13] G. Gutierrez,[45]
P. Gutierrez,[67] J. Haley,[68] L. Han,[4] K. Harder,[41] A. Harel,[63] J.M. Hauptman,[52] J. Hays,[40] T. Head,[41]
T. Hebbeker,[18] D. Hedin,[47] H. Hegab,[68] A.P. Heinson,[43] U. Heintz,[69] C. Hensel,[1] I. Heredia-De La Cruz[d],[28]
K. Herner,[45] G. Hesketh[f],[41] M.D. Hildreth,[51] R. Hirosky,[73] T. Hoang,[44] J.D. Hobbs,[64] B. Hoeneisen,[9] J. Hogan,[72]
M. Hohlfeld,[21] J.L. Holzbauer,[58] I. Howley,[70] Z. Hubacek,[7,15] V. Hynek,[7] I. Iashvili,[62] Y. Ilchenko,[71]
R. Illingworth,[45] A.S. Ito,[45] S. Jabeen[m],[45] M. Jaffré,[13] A. Jayasinghe,[67] M.S. Jeong,[27] R. Jesik,[40] P. Jiang,[4]
K. Johns,[42] E. Johnson,[57] M. Johnson,[45] A. Jonckheere,[45] P. Jonsson,[40] J. Joshi,[43] A.W. Jung,[45] A. Juste,[36]
E. Kajfasz,[12] D. Karmanov,[33] I. Katsanos,[59] M. Kaur,[23] R. Kehoe,[71] S. Kermiche,[12] N. Khalatyan,[45] A. Khanov,[68]
A. Kharchilava,[62] Y.N. Kharzheev,[31] I. Kiselevich,[32] J.M. Kohli,[23] A.V. Kozelov,[34] J. Kraus,[58] A. Kumar,[62]
A. Kupco,[8] T. Kurča,[17] V.A. Kuzmin,[33] S. Lammers,[49] P. Lebrun,[17] H.S. Lee,[27] S.W. Lee,[52] W.M. Lee,[45] X. Lei,[42]
J. Lellouch,[14] D. Li,[14] H. Li,[73] L. Li,[43] Q.Z. Li,[45] J.K. Lim,[27] D. Lincoln,[45] J. Linnemann,[57] V.V. Lipaev,[34]
R. Lipton,[45] H. Liu,[71] Y. Liu,[4] A. Lobodenko,[35] M. Lokajicek,[8] R. Lopes de Sa,[45] R. Luna-Garcia[g],[28]
A.L. Lyon,[45] A.K.A. Maciel,[1] R. Madar,[19] R. Magaña-Villalba,[28] S. Malik,[59] V.L. Malyshev,[31] J. Mansour,[20]
J. Martínez-Ortega,[28] R. McCarthy,[64] C.L. McGivern,[41] M.M. Meijer,[29,30] A. Melnitchouk,[45] D. Menezes,[47]
P.G. Mercadante,[3] M. Merkin,[33] A. Meyer,[18] J. Meyer[i],[20] F. Miconi,[16] N.K. Mondal,[25] M. Mulhearn,[73] E. Nagy,[12]
M. Narain,[69] R. Nayyar,[42] H.A. Neal,[56] J.P. Negret,[5] P. Neustroev,[35] H.T. Nguyen,[73] T. Nunnemann,[22]
J. Orduna,[72] N. Osman,[12] J. Osta,[51] A. Pal,[70] N. Parashar,[50] V. Parihar,[69] S.K. Park,[27] R. Partridge[e],[69]
N. Parua,[49] A. Patwa[j],[65] B. Penning,[45] M. Perfilov,[33] Y. Peters,[41] K. Petridis,[41] G. Petrillo,[63] P. Pétroff,[13]
M.-A. Pleier,[65] V.M. Podstavkov,[45] A.V. Popov,[34] M. Prewitt,[72] D. Price,[41] N. Prokopenko,[34] J. Qian,[56]
A. Quadt,[20] B. Quinn,[58] P.N. Ratoff,[39] I. Razumov,[34] I. Ripp-Baudot,[16] F. Rizatdinova,[68] M. Rominsky,[45]
A. Ross,[39] C. Royon,[15] P. Rubinov,[45] R. Ruchti,[51] G. Sajot,[11] A. Sánchez-Hernández,[28] M.P. Sanders,[22]
A.S. Santos[h],[1] G. Savage,[45] M. Savitskyi,[38] L. Sawyer,[54] T. Scanlon,[40] R.D. Schamberger,[64] Y. Scheglov,[35]
H. Schellman,[48] C. Schwanenberger,[41] R. Schwienhorst,[57] J. Sekaric,[53] H. Severini,[67] E. Shabalina,[20] V. Shary,[15]
S. Shaw,[41] A.A. Shchukin,[34] V. Simak,[7] P. Skubic,[67] P. Slattery,[63] D. Smirnov,[51] G.R. Snow,[59] J. Snow,[66]
S. Snyder,[65] S. Söldner-Rembold,[41] L. Sonnenschein,[18] K. Soustruznik,[6] J. Stark,[11] D.A. Stoyanova,[34] M. Strauss,[67]
L. Suter,[41] P. Svoisky,[67] M. Titov,[15] V.V. Tokmenin,[31] Y.-T. Tsai,[63] D. Tsybychev,[64] B. Tuchming,[15] C. Tully,[61]
L. Uvarov,[35] S. Uvarov,[35] S. Uzunyan,[47] R. Van Kooten,[49] W.M. van Leeuwen,[29] N. Varelas,[46] E.W. Varnes,[42]
I.A. Vasilyev,[34] A.Y. Verkheev,[31] L.S. Vertogradov,[31] M. Verzocchi,[45] M. Vesterinen,[41] D. Vilanova,[15] P. Vokac,[7]
H.D. Wahl,[44] M.H.L.S. Wang,[45] J. Warchol,[51] G. Watts,[74] M. Wayne,[51] J. Weichert,[21] L. Welty-Rieger,[48]
M.R.J. Williams[n],[49] G.W. Wilson,[53] M. Wobisch,[54] D.R. Wood,[55] T.R. Wyatt,[41] Y. Xie,[45] R. Yamada,[45]

S. Yang,[4] T. Yasuda,[45] Y.A. Yatsunenko,[31] W. Ye,[64] Z. Ye,[45] H. Yin,[45] K. Yip,[65] S.W. Youn,[45] J.M. Yu,[56]
J. Zennamo,[62] T.G. Zhao,[41] B. Zhou,[56] J. Zhu,[56] M. Zielinski,[63] D. Zieminska,[49] and L. Zivkovic[14]

(The D0 Collaboration[*])

[1]LAFEX, Centro Brasileiro de Pesquisas Físicas, Rio de Janeiro, Brazil
[2]Universidade do Estado do Rio de Janeiro, Rio de Janeiro, Brazil
[3]Universidade Federal do ABC, Santo André, Brazil
[4]University of Science and Technology of China, Hefei, People's Republic of China
[5]Universidad de los Andes, Bogotá, Colombia
[6]Charles University, Faculty of Mathematics and Physics,
Center for Particle Physics, Prague, Czech Republic
[7]Czech Technical University in Prague, Prague, Czech Republic
[8]Institute of Physics, Academy of Sciences of the Czech Republic, Prague, Czech Republic
[9]Universidad San Francisco de Quito, Quito, Ecuador
[10]LPC, Université Blaise Pascal, CNRS/IN2P3, Clermont, France
[11]LPSC, Université Joseph Fourier Grenoble 1, CNRS/IN2P3,
Institut National Polytechnique de Grenoble, Grenoble, France
[12]CPPM, Aix-Marseille Université, CNRS/IN2P3, Marseille, France
[13]LAL, Université Paris-Sud, CNRS/IN2P3, Orsay, France
[14]LPNHE, Universités Paris VI and VII, CNRS/IN2P3, Paris, France
[15]CEA, Irfu, SPP, Saclay, France
[16]IPHC, Université de Strasbourg, CNRS/IN2P3, Strasbourg, France
[17]IPNL, Université Lyon 1, CNRS/IN2P3, Villeurbanne, France and Université de Lyon, Lyon, France
[18]III. Physikalisches Institut A, RWTH Aachen University, Aachen, Germany
[19]Physikalisches Institut, Universität Freiburg, Freiburg, Germany
[20]II. Physikalisches Institut, Georg-August-Universität Göttingen, Göttingen, Germany
[21]Institut für Physik, Universität Mainz, Mainz, Germany
[22]Ludwig-Maximilians-Universität München, München, Germany
[23]Panjab University, Chandigarh, India
[24]Delhi University, Delhi, India
[25]Tata Institute of Fundamental Research, Mumbai, India
[26]University College Dublin, Dublin, Ireland
[27]Korea Detector Laboratory, Korea University, Seoul, Korea
[28]CINVESTAV, Mexico City, Mexico
[29]Nikhef, Science Park, Amsterdam, the Netherlands
[30]Radboud University Nijmegen, Nijmegen, the Netherlands
[31]Joint Institute for Nuclear Research, Dubna, Russia
[32]Institute for Theoretical and Experimental Physics, Moscow, Russia
[33]Moscow State University, Moscow, Russia
[34]Institute for High Energy Physics, Protvino, Russia
[35]Petersburg Nuclear Physics Institute, St. Petersburg, Russia
[36]Institució Catalana de Recerca i Estudis Avançats (ICREA) and Institut de Física d'Altes Energies (IFAE), Barcelona, Spain
[37]Uppsala University, Uppsala, Sweden
[38]Taras Shevchenko National University of Kyiv, Kiev, Ukraine
[39]Lancaster University, Lancaster LA1 4YB, United Kingdom
[40]Imperial College London, London SW7 2AZ, United Kingdom
[41]The University of Manchester, Manchester M13 9PL, United Kingdom
[42]University of Arizona, Tucson, Arizona 85721, USA
[43]University of California Riverside, Riverside, California 92521, USA
[44]Florida State University, Tallahassee, Florida 32306, USA
[45]Fermi National Accelerator Laboratory, Batavia, Illinois 60510, USA
[46]University of Illinois at Chicago, Chicago, Illinois 60607, USA
[47]Northern Illinois University, DeKalb, Illinois 60115, USA
[48]Northwestern University, Evanston, Illinois 60208, USA
[49]Indiana University, Bloomington, Indiana 47405, USA
[50]Purdue University Calumet, Hammond, Indiana 46323, USA
[51]University of Notre Dame, Notre Dame, Indiana 46556, USA
[52]Iowa State University, Ames, Iowa 50011, USA
[53]University of Kansas, Lawrence, Kansas 66045, USA
[54]Louisiana Tech University, Ruston, Louisiana 71272, USA
[55]Northeastern University, Boston, Massachusetts 02115, USA
[56]University of Michigan, Ann Arbor, Michigan 48109, USA
[57]Michigan State University, East Lansing, Michigan 48824, USA
[58]University of Mississippi, University, Mississippi 38677, USA

^{59}University of Nebraska, Lincoln, Nebraska 68588, USA
^{60}Rutgers University, Piscataway, New Jersey 08855, USA
^{61}Princeton University, Princeton, New Jersey 08544, USA
^{62}State University of New York, Buffalo, New York 14260, USA
^{63}University of Rochester, Rochester, New York 14627, USA
^{64}State University of New York, Stony Brook, New York 11794, USA
^{65}Brookhaven National Laboratory, Upton, New York 11973, USA
^{66}Langston University, Langston, Oklahoma 73050, USA
^{67}University of Oklahoma, Norman, Oklahoma 73019, USA
^{68}Oklahoma State University, Stillwater, Oklahoma 74078, USA
^{69}Brown University, Providence, Rhode Island 02912, USA
^{70}University of Texas, Arlington, Texas 76019, USA
^{71}Southern Methodist University, Dallas, Texas 75275, USA
^{72}Rice University, Houston, Texas 77005, USA
^{73}University of Virginia, Charlottesville, Virginia 22904, USA
^{74}University of Washington, Seattle, Washington 98195, USA
(Dated: April 27, 2015)

We measure the forward-backward asymmetry in the production of Λ_b^0 and $\overline{\Lambda}_b^0$ baryons as a function of rapidity in $p\overline{p}$ collisions at $\sqrt{s} = 1.96$ TeV using 10.4 fb^{-1} of data collected with the D0 detector at the Fermilab Tevatron collider. The asymmetry is determined by the preference of Λ_b^0 or $\overline{\Lambda}_b^0$ particles to be produced in the direction of the beam protons or antiprotons, respectively. The measured asymmetry integrated over rapidity y in the range $0.1 < |y| < 2.0$ is $A = 0.04 \pm 0.07\,(\mathrm{stat}) \pm 0.02\,(\mathrm{syst})$.

Hadroproduction of particles carrying a heavy quark Q ($Q = b, c$) proceeds through gluon-gluon fusion or quark-antiquark annihilations [1], followed by hadronization of the heavy quarks. At the parton level of leading-order (LO) quantum chromodynamics (QCD), Q and $\overline{Q}$ quarks are produced symmetrically. Next-to-leading order (NLO) QCD effects can introduce a small asymmetry of $\approx 1\%$ in Q and $\overline{Q}$ momenta from interfering amplitudes. The hadronization process may also change the direction of the particle carrying the quark Q relative to the original Q direction and thus generate a significant asymmetry.

There have been few studies of this effect in bottom baryon production compared to bottom mesons. Production of heavy baryons is sensitive to effects of nonperturbative final state interactions of a QCD string connecting the b quark and a remnant of the proton. The production of the ground-state bottom baryon Λ_b^0 and

———

*with visitors from ^{a}Augustana College, Sioux Falls, SD, USA, ^{b}The University of Liverpool, Liverpool, UK, ^{c}DESY, Hamburg, Germany, ^{d}CONACyT, Mexico City, Mexico, ^{e}SLAC, Menlo Park, CA, USA, ^{f}University College London, London, UK, ^{g}Centro de Investigacion en Computacion - IPN, Mexico City, Mexico, ^{h}Universidade Estadual Paulista, São Paulo, Brazil, ^{i}Karlsruher Institut für Technologie (KIT) - Steinbuch Centre for Computing (SCC), D-76128 Karlsruhe, Germany, ^{j}Office of Science, U.S. Department of Energy, Washington, D.C. 20585, USA, ^{k}American Association for the Advancement of Science, Washington, D.C. 20005, USA, ^{l}Kiev Institute for Nuclear Research, Kiev, Ukraine, ^{m}University of Maryland, College Park, Maryland 20742, USA and ^{n}European Orgnaization for Nuclear Research (CERN), Geneva, Switzerland

its antiparticle $\overline{\Lambda}_b^0$ has been recently discussed by Rosner [2], who proposes the "string drag" mechanism that may favor production of Λ_b^0 baryons in the hemisphere containing the beam proton, and $\overline{\Lambda}_b^0$ baryons in the antiproton beam hemisphere. In the string drag picture, the QCD interaction between a b quark produced in the $p\overline{p}$ collision and the remnant of the proton is described by a string with a linear potential. When the string breaks, it imparts an impulse to the quark along the beam axis. Assuming a string tension of 0.18 GeV^2, Rosner made an approximate prediction for the shift in the particle longitudinal momentum relative to the axis along the beam direction of $\Delta p_z = 1.4$ GeV, resulting in a shift in rapidity of approximately $\Delta y = 1.4$ GeV$/E$, where E is the energy of the particle and the rapidity is defined as $y = \ln((E + p_z)/(E - p_z))/2$. Another possible source of asymmetry in Λ_b^0 production is the coalescence of an intrinsic b quark at large momentum fraction x in the Fock state $|uudb\overline{b}\rangle$ of the proton with a comoving diquark ud from the proton [3].

In this article, we present a study of the forward-backward production asymmetry of Λ_b^0 and $\overline{\Lambda}_b^0$ baryons using the fully reconstructed decay chain $\Lambda_b^0 \to J/\psi\Lambda$, $J/\psi \to \mu^+\mu^-$, $\Lambda \to p\pi^-$, and its charge conjugate. The forward (F) category corresponds to a particle (Λ_b^0 or $\overline{\Lambda}_b^0$) sharing valence quark flavors with a beam particle with the same sign of rapidity, and the backward (B) category corresponds to the reverse association. In $p\overline{p}$ collisions at D0, we choose the positive z-axis to be in the direction of the proton beam, so that the forward direction corresponds to a Λ_b^0 particle emitted with $y > 0$ or a $\overline{\Lambda}_b^0$ particle emitted at $y < 0$. In pp collisions, Λ_b^0

particles are assigned to the forward category and $\overline{\Lambda}_b^0$ particles to the backward category. To facilitate a comparison with existing measurements, we present the ratio of the backward to forward production cross sections, $R = \sigma(B)/\sigma(F)$, and the forward-backward asymmetry, $A = (\sigma(F) - \sigma(B))/(\sigma(F) + \sigma(B))$, as functions of the rapidity y. The data sample corresponds to an integrated luminosity of 10.4 fb^{-1} collected with the D0 detector in $p\bar{p}$ collisions at $\sqrt{s} = 1.96$ TeV at the Fermilab Tevatron collider.

Using the same data set, the D0 experiment has studied the forward-backward asymmetry in the production of $B^{\pm}$ mesons, observing no rapidity dependence [4]. The measured forward-backward asymmetry in the production of $B^{\pm}$ mesons, where the forward category corresponds to B^- mesons produced at $y > 0$ and B^+ mesons produced at $y < 0$, is $A_{\mathrm{FB}}(B^{\pm}) = [-0.24 \pm 0.41\,(\mathrm{stat}) \pm 0.19\,(\mathrm{syst})]\%$, integrated over rapidity.

The D0 detector consists of a central tracking system, calorimeters, and muon detectors [5]. The central tracking system comprises a silicon microstrip tracker and a central fiber tracker, both located inside a 1.9 T superconducting solenoidal magnet. The tracking system is designed to optimize tracking and vertexing for pseudorapidities $|\eta| < 3$, where $\eta = -\ln[\tan(\theta/2)]$, and θ is the polar angle with respect to the proton beam direction. The tracking system can reconstruct the primary $p\bar{p}$ interaction vertex for interactions with at least three secondary tracks with a precision of $\approx 35\ \mu$m ($\approx 90\ \mu$m) in the plane transverse to (along) the beam direction. The muon detector, positioned outside the calorimeter, consists of a central muon system covering the pseudorapidity region of $|\eta| < 1$ and a forward muon system covering the pseudorapidity region of $1 < |\eta| < 2$. Both central and forward systems consist of a layer of drift tubes and scintillators inside 1.8 T iron toroidal magnets and two similar layers outside the toroids [6]. The toroid and solenoid magnet polarities were periodically reversed, allowing for a cancellation of first-order effects related to a possible instrumental asymmetry.

Candidate events are required to include a pair of oppositely charged muons. At least one muon is required to be detected in the muon chambers in front of and behind a toroid magnet. The other muon may be detected only in front of the toroid or as a minimum ionizing particle in the calorimeter. Each muon candidate is required to match a track found in the central tracking system.

To form Λ_b^0 and $\overline{\Lambda}_b^0$ candidates, muon pairs in the invariant mass range $2.9 < M(\mu^+\mu^-) < 3.3$ GeV, consistent with a J/ψ meson decay, are combined with Λ baryon candidates. The Λ candidates are formed from pairs of oppositely charged tracks originating from a common vertex, consistent with a decay $\Lambda \to p\pi^-$ or $\overline{\Lambda} \to \bar{p}\pi^+$. The charged particle with the higher momentum is assigned the proton mass. A previous analysis has shown that the misassignment of the proton track is negligible [7]. The Λ candidate is required to have an invariant mass between 1.107 and 1.125 GeV and a transverse momentum greater than 1.8 GeV. The separation of the Λ decay vertex from the primary vertex in the transverse plane must be between 0.5 and 25 cm. A kinematic fit of the parameters of tracks forming the Λ_b^0 candidate is performed by constraining the dimuon invariant mass to the world-average J/ψ mass [8], and constraining the $J/\psi\Lambda$ system to originate from a common decay vertex. The modified track parameters are used in the calculation of the Λ_b^0 invariant mass. We require $5.0 < M(J/\psi\Lambda) < 6.2$ GeV.

To suppress the large background from prompt J/ψ production, we require a significant separation of the Λ_b^0 decay vertex from the primary vertex. To reconstruct the primary vertex, tracks are selected that do not belong to the Λ_b^0 decay. We constrain the transverse position of the primary vertex to the average beam location in the transverse plane. We define the signed decay length of a Λ_b^0 baryon, L_{xy}, as the vector pointing from the primary vertex to the Λ_b^0 decay vertex projected on the direction of the Λ_b^0 transverse momentum $\vec{p}_T$. We require L_{xy} to be greater than three times its uncertainty.

The mass distributions for Λ_b^0 candidates in the range $0.5 < |y| < 1.0$ in the forward and backward categories are shown in Fig. 1. Binned maximum-likelihood fits of a Gaussian signal function and a second-order Chebyshev polynomial for the background yield a forward (backward) signal with a mean mass of $M(\Lambda_b^0) = 5618.1 \pm 4.3$ MeV (5619.9 ± 4.7 MeV), consistent with the world-average Λ_b^0 mass [8]. The width depends on y and varies between about 30 and 50 MeV. The average reconstructed p_T of Λ_b^0 candidates is $\langle p_T \rangle = 9.9$ GeV after background subtraction.

The production rates of forward and backward Λ_b^0 and $\overline{\Lambda}_b^0$ baryons are extracted from fits to the invariant mass distributions of forward and backward candidates in four rapidity bins in the range $0.1 < |y| < 2.0$, as defined in Table I. We reject the region $|y| < 0.1$ where the asymmetry may be diluted by forward-backward migration due to the finite polar angle resolution [4].

Samples of fully simulated Monte Carlo (MC) signal events are obtained at LO with PYTHIA [9] and at NLO with MC@NLO [10], using the parton distribution function sets CTEQ6L1 and CTEQ6M1 [11], respectively. PYTHIA generates $b\bar{b}$ quark pairs via direct $2 \to 2$ processes ($q_i\bar{q}_i, gg \to b\bar{b}$) and decays of gauge bosons, as well as through flavor excitation processes like $bg \to bg$, and gluon splittings, $g \to b\bar{b}$. The event generator MC@NLO is interfaced with HERWIG [12] for parton showering and hadronization. After hadronization, bottom hadron decays are simulated with EVTGEN [13]. In the simulation, the Λ_b^0 and $\overline{\Lambda}_b^0$ baryons are forced to decay to $J/\psi\Lambda$, $J/\psi \to \mu^+\mu^-$, using the phase space (PHSP) and vector to lepton-lepton (VLL) models in EVTGEN. The detector response is simulated with GEANT3 [14] and multiple $p\bar{p}$ interactions (pileup) are modeled by overlaying hits from random bunch crossings in data. A MC sample generated with PYTHIA, 30 times the number of signal events in the data sample, is used to obtain efficiencies

TABLE I: Efficiencies ϵ, averaged values of background-subtracted transverse momenta $\langle p_T \rangle$, backward and forward fitted yields for the signal $N(B)$ and $N(F)$, forward-backward asymmetries A, and cross-section ratios R in four intervals of rapidity. Uncertainties on $\langle p_T \rangle$, $N(B)$ and $N(F)$ are statistical only. Uncertainties on ϵ arise from the statistical precision of the simulated event samples.

$|y|$	ϵ (%)	$\langle p_T \rangle$ (GeV)	$N(B)$	$N(F)$	$A \pm$ (stat) $\pm$ (syst)	$R \pm$ (stat) $\pm$ (syst)
$0.1-0.5$	0.70 ± 0.01	10.2 ± 0.1	125 ± 18	92 ± 17	$-0.15 \pm 0.11 \pm 0.03$	$1.36 \pm 0.32 \pm 0.06$
$0.5-1.0$	1.01 ± 0.01	10.0 ± 0.1	135 ± 19	154 ± 22	$0.07 \pm 0.10 \pm 0.02$	$0.88 \pm 0.18 \pm 0.04$
$1.0-1.5$	0.97 ± 0.01	9.7 ± 0.1	123 ± 16	158 ± 23	$0.12 \pm 0.10 \pm 0.02$	$0.78 \pm 0.15 \pm 0.04$
$1.5-2.0$	0.32 ± 0.01	9.8 ± 0.2	22 ± 9	33 ± 10	$0.21 \pm 0.24 \pm 0.02$	$0.67 \pm 0.34 \pm 0.03$
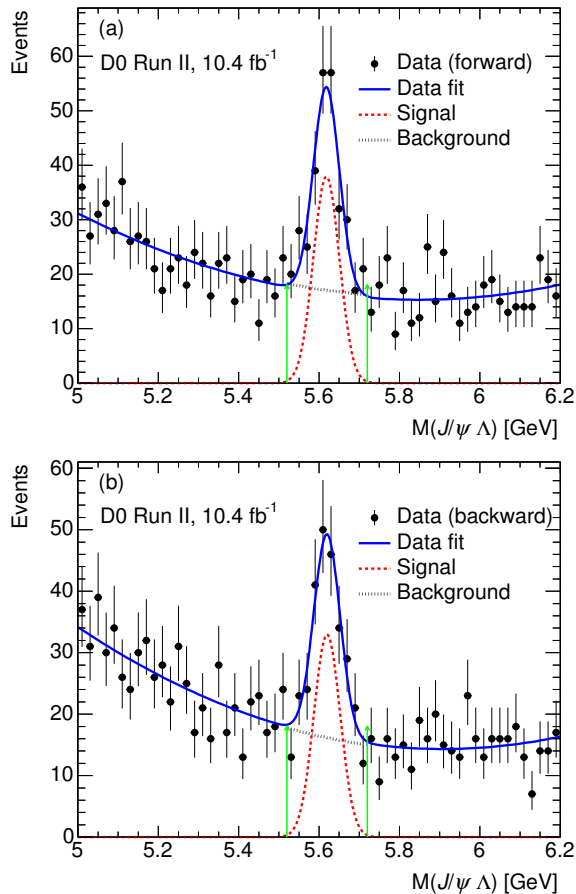
FIG. 1: (color online) Invariant mass distribution of $\Lambda_b^0 \to J/\psi \Lambda$ and $\overline{\Lambda}_b^0 \to J/\psi \overline{\Lambda}$ candidates in the rapidity range $0.5 < |y| < 1.0$ in the (a) forward and (b) backward categories. The fit of a Gaussian signal function with a second-order Chebyshev polynomial background function is superimposed. The vertical lines define the signal region.

for reconstructing Λ_b^0 baryons in each of the four rapidity intervals shown in Table I. The Λ_b^0 efficiencies are suppressed by the large transverse momentum requirement on the Λ candidates and by the low reconstruction efficiency for the long-lived Λ baryon.

Most of the systematic uncertainties in the production cross-sections of Λ_b^0 and $\overline{\Lambda}_b^0$ baryons arise from uncertain-

TABLE II: Systematic uncertainties (in %) on the measurement of the backward-to-forward ratio R.

Source	Uncertainty (%)
Signal shape	2
Background shape	2
Detection efficiency	3
Total syst. uncertainty	4

ties in the kinematic acceptance and detection efficiency of final-state particles and cancel in the measurements of the asymmetry A and ratio R. The remaining uncertainties are due to the signal and background shapes assumed in the mass fits and the different efficiencies of forward and backward particle reconstruction. The uncertainty from the signal shape is estimated by comparing the results of the central fits with the results obtained when the width parameters for the forward and backward categories are constrained to be equal. The sensitivity to the background shape is estimated by increasing the lower mass requirement to $M(J/\psi\Lambda) > 5.2$ GeV, thus excluding the mass range where feed-down from multi-body bottom baryon decays may be present. The estimate of the uncertainty on the detection efficiency is based on the average deviation from unity of the ratio R of reconstructed events in four rapidity intervals for a sample of MC events generated with no asymmetry. Adding the uncertainties in quadrature results in a total systematic uncertainty of $\pm4\%$. The systematic uncertainties are summarized in Table II.

The fitted signal yields and the resulting forward-backward asymmetry A are presented in Table I. We observe that there is a weak correlation between rapidity y and the averaged value of background-subtracted transverse momentum $\langle p_T \rangle$ of Λ_b^0 candidates. The asymmetry integrated over $|y|$, taking into account the rapidity dependent efficiency ϵ, is $A = 0.04 \pm 0.07\,\text{(stat)} \pm 0.02\,\text{(syst)}$.

The forward-backward asymmetry as a function of $|y|$ is shown in Fig. 2. There is a wide range of model predictions for this asymmetry. The "heavy quark recombination" model [15], as shown in Fig. 2, predicts a modest asymmetry, reaching $\approx 2\%$ near $|y| = 2$. While PYTHIA predicts no asymmetry, the MC@NLO generator inter-
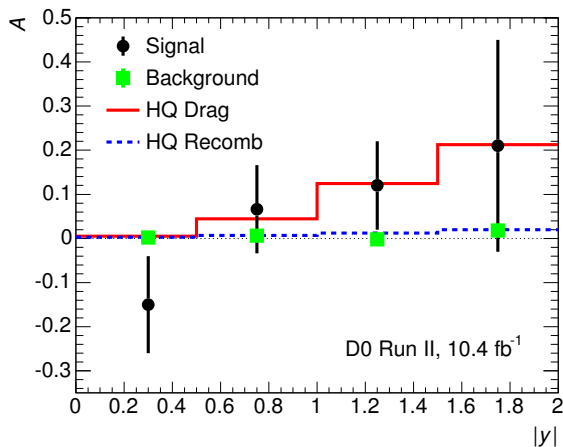
FIG. 2: (color online) Measured forward-backward asymmetry A versus rapidity $|y|$ compared to predictions of the heavy quark recombination model [15] and a simulated effect of the longitudinal momentum shift due to beam drag (see Ref. [2] and text). The background asymmetry is obtained from $J/\psi\Lambda$ candidates in the Λ_b^0 mass sidebands (uncertainties are small compared to the symbol size). Measurements are placed at the centers of the rapidity intervals defined in Table I.

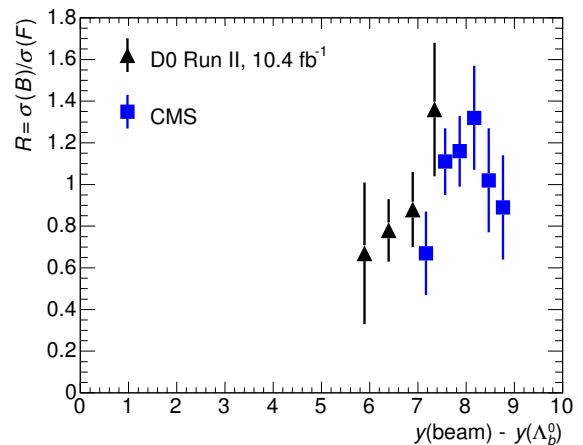FIG. 3: Measured ratio of the backward to forward production cross sections versus rapidity loss compared to the $\overline{\Lambda}_b^0$ to Λ_b^0 production cross section ratio at CMS taken from Table II of Ref. [16]. Measurements are placed at the centers of their rapidity loss ranges.

faced with HERWIG predicts a large asymmetry, reaching 100% close to $|y| = 2$. Our results are consistent with no asymmetry within the large uncertainties, although they show a trend of increasing asymmetry with increasing $|y|$ that could be interpreted as the effect of the longitudinal momentum imparted to a Λ_b^0 or $\overline{\Lambda}_b^0$ particle by the beam remnant. Assuming a shift of $\Delta p_z = 1.4$ GeV in the particle longitudinal momentum, as estimated by Rosner [2], we have simulated the effect by adding 1.4 GeV (-1.4 GeV) to the Λ_b^0 ($\overline{\Lambda}_b^0$) baryon p_z in the generated PYTHIA events. As shown in Fig. 2, our result is in a good agreement with this prediction. We find our results in disagreement with the large asymmetry predicted by MC@NLO+HERWIG.

The results for the backward-to-forward ratio R for the same rapidity intervals are given in Table I and shown in Fig. 3, where we compare with the results for the ratio of cross sections, $\sigma(\overline{\Lambda}_b^0)/\sigma(\Lambda_b^0)$, for the six rapidity bins reported by the CMS Collaboration [16]. All results are presented as functions of the "rapidity loss", defined as the difference between the rapidity of the beam, $y(\text{beam}) = 7.64$ (8.92) at the Tevatron (LHC), and the rapidity y of the Λ_b^0 baryon. The D0 and CMS results are consistent within large uncertainties. Together, they show a trend of R to fall with increasing rapidity and decreasing rapidity loss. The D0 result for the ratio R integrated over rapidity, taking into account the rapidity dependent efficiency ϵ, is $R = 0.92 \pm 0.12\,(\text{stat}) \pm 0.04\,(\text{syst})$, to be compared with the value of $R = 1.02 \pm 0.07\,(\text{stat}) \pm 0.09\,(\text{syst})$ reported by the CMS Collaboration.

In order to verify that detector effects on R and A

are not significant, the analysis was repeated considering candidates with $y > 0$ (or $y < 0$) only, and Λ_b^0 (or $\overline{\Lambda}_b^0$) only. Within statistical uncertainties, all results are consistent with each other and with the measurements listed in Table I. Furthermore, as shown in Fig. 2, we find a negligible forward-backward asymmetry in the four intervals of rapidity in a sample of background candidates obtained from the Λ_b^0 mass sidebands (region above and below the Λ_b^0 signal region defined in Fig. 1) with no L_{xy} requirement.

In summary, we have presented a measurement of the forward-backward asymmetry in the production of Λ_b^0 and $\overline{\Lambda}_b^0$ baryons as a function of rapidity $|y|$. Together with related results from the LHC, the data show a tendency of forward particles that share valence quarks with beam remnants, to be emitted at larger values of rapidity, corresponding to smaller rapidity loss, than their backward counterparts. The measured ratio of the backward-to-forward production rate at the mean transverse momentum of $\langle p_T \rangle = 9.9$ GeV, averaged over rapidity in the range $0.1 < |y| < 2.0$, is $R = 0.92 \pm 0.12\,(\text{stat}) \pm 0.04\,(\text{syst})$. The measured forward-backward asymmetry is $A = 0.04 \pm 0.07\,(\text{stat}) \pm 0.02\,(\text{syst})$.

[1] P. Nason, S. Dawson and R. K. Ellis, The total cross-section for the production of heavy quarks in hadronic collisions, Nucl. Phys. **B303**, 607 (1988).

[2] J. L. Rosner, Asymmetry in Λ_b and $\overline{\Lambda}_b$ production, Phys. Rev. D **90**, 014023 (2014).

[3] S. J. Brodsky, *Novel Perspectives for Hadron Physics, Subnuclear Physics: Past, Present and Future*, Pontifical Academy of Sciences, Scripta Varia 119, Vatican City, 2014.

[4] V. M. Abazov *et al.* (D0 Collaboration), Measurement of the forward-backward asymmetry in the production of $B^{\pm}$ mesons in $p\bar{p}$ collisions at $\sqrt{s} = 1.96$ TeV, Phys. Rev. Lett. **114**, 051803 (2015).

[5] V. M. Abazov *et al.* (D0 Collaboration), The upgraded D0 detector, Nucl. Instrum. Methods Phys. Res., Sect. A **565**, 463 (2006).

[6] V. M. Abazov *et al.* (D0 Collaboration), The muon system of the Run II D0 detector, Nucl. Instrum. Methods Phys. Res. A **552**, 372 (2005).

[7] V. M. Abazov *et al.* (D0 Collaboration), Measurement of the Λ_b^0 lifetime in the exclusive decay $\Lambda_b^0 \to J/\psi\Lambda^0$ in $p\bar{p}$ collisions at $\sqrt{s} = 1.96$ TeV, Phys. Rev. D **85**, 112003 (2012).

[8] K. A. Olive *et al.*, Review of particle physics, Chin. Phys. C **38**, 090001 (2014).

[9] T. Sjöstrand *et al.* , High-energy physics event generation with PYTHIA 6.1, Comp. Phys. Commun. **135**, 238 (2001).

[10] S. Frixione and B. R. Webber, Matching NLO QCD computations and parton shower simulations, J. High Energy Phys. 06 (2002) 029; S. Frixione, P. Nason and B. R. Webber, Matching NLO QCD and parton showers in heavy flavor production, J. High Energy Phys. 08 (2003) 007.

[11] J. Pumplin *et al.*, New generation of parton distributions with uncertainties from global QCD analysis, J. High Energy Phys. 07 (2002) 012; D. Stump *et al.*, Inclusive jet production, parton distributions, and the search for new physics, J. High Energy Phys. 10 (2003) 046.

[12] G. Corcella *et al.*, Herwig 6: an event generator for hadron emission reactions with interfering gluons (including supersymmetric processes), J. High Energy Phys. 01 (2001) 010.

[13] D. J. Lange, The EvtGen particle simulation package, Nucl. Instrum. Meth. Phys. Res. Sect. A **462**, 152 (2001).

[14] R. Brun and F. Carminati, GEANT – Detector Description and Simulation Tool, CERN Program Library Long Writeup No. W5013, 1993 (unpublished).

[15] W. K. Lai and A. K. Leibovich, Λ_c^+/Λ_c^- and $\Lambda_b^0/\bar{\Lambda}_b^0$ production asymmetry at the LHC from heavy quark recombination, Phys. Rev. D **91**, 054022 (2015) and private communications.

[16] S. Chatrchyan *et al.* (CMS Collaboration), Measurement of the Λ_b cross section and the $\bar{\Lambda}_b$ to Λ_b ratio with $J/\psi\Lambda$ decays in pp collisions at $\sqrt{s} = 7$ TeV, Phys. Lett. B **714**, 136 (2012) .